Tolerogenic propreties of liver macrophages in non-alcoholic steatohepatitis

Orci, Lorenzo; Kreutzfeldt, Mario; Goossens, Nicolas; Rubbia-Brandt, Laura; Slits, Florence; Hammad, Karim; Delaune, Vaihere; Oldani, Graziano; Negro, Francesco; Clément Leboube, Sophie; Gonelle-Gispert, Carmen; Buehler, Leo Hans; Toso, Christian; Lacotte, Stéphanie

How to cite

ORCI, Lorenzo et al. Tolerogenic propreties of liver macrophages in non-alcoholic steatohepatitis. In: Liver International, 2019. doi: 10.1111/liv.14336

This publication URL: https://archive-ouverte.unige.ch/unige:128391

Publication DOI: 10.1111/liv.14336

DR. LORENZO ANNIBAL ORCI (Orcid ID : 0000-0002-7540-198X)
DR. NICOLAS GOOSSENS (Orcid ID : 0000-0002-8698-4690)
DR. FRANCESCO NEGRO (Orcid ID : 0000-0003-4046-4806)

Article type : Original Articles
Editor : Gabriele Missale

Tolerogenic propreties of liver macrophages in non-alcoholic steatohepatitis

Lorenzo A. Orci[1, 2], Mario Kreutzfeldt [3, 4], Nicolas Goossens [2, 5], Laura Rubbia-Brandt [2, 3, 4], Florence Slits [1], Karim Hammad [3], Vaihere Delaune [1, 2], Graziano Oldani [1, 2], Francesco Negro [3, 4], Sophie Clément [3], Carmen Gonelle-Gispert [1], Léo H. Buhler [1], Christian Toso [1, 2], Stéphanie Lacotte [1]

[1] Division of Abdominal and Transplantation Surgery, Department of Surgery, Geneva University Hospitals and Faculty of Medicine, Switzerland.

[2] Hepato-pancreato-biliary centre, Geneva University Hospitals and Faculty of Medicine, Switzerland.

[3] Department of Pathology and Immunology, University of Geneva, Geneva, Switzerland

[4] Division of Clinical Pathology, Geneva University Hospital, Switzerland.

[5] Division of Gastroenterology and Hepatology, Department of Medicine, Geneva University Hospitals and Faculty of Medicine, Switzerland.

Corresponding author: Dr Lorenzo Orci, MD-PhD, Division of Abdominal and Transplantation Surgery, Department of Surgery, Geneva University Hospitals and Faculty of Medicine, 4 rue Gabrielle-Perret-Gentil, 1211 Geneva, Switzerland. Tel: +41223723311 Email: Lorenzo.orci@hcuge.ch

Word count (including title, lay summary, abstract, main text and references): 5453. Total number of figures and Tables: 7 and 1. Number of supplementary Figures and table: 4 and 1.

Abbreviations: Non-alcoholic fatty liver disease (NAFLD), Non-alcoholic steatohepatitis (NASH), Cluster of differentiation (CD), Programmed-death ligand 1 (PD-L1), steatosis, activity and fibrosis score (SAF score), Gene set enrichment analysis (GSEA), Major histocompatibility complex (MHC), Carbon tetrachloride (CCL4), Hepatitis B virus (HBV).

The authors declare have no conflict of interest to disclose. Financial support: This study was supported by grants from the Swiss National Science Foundation (323530–151477, PP00P3_139021), the Geneva Cancer League (ref 1509), the Minkoff Foundation, the Artères Foundation, and the Insuleman Foundation.

Acknowledgments: We would like to thank Dr Yannick Müller for his critical review of the manuscript, and Mr. Julien Charbon for his assistance in data analysis

ABSTRACT

Background & Aims: Our understanding of non-alcoholic fatty liver disease (NAFLD) pathogenesis is improving, but there is still limited data on the function of resident liver macrophages in this context, especially when considering their contribution in dampening liver inflammation.

Methods: Liver macrophages were studied in mouse models of prolonged diet-induced liver steatohepatitis and carbon tetrachloride-induced liver injury. We assessed liver macrophages phenotype and co-stimulatory/inhibitory properties upon exposure to lipopolysaccharide or interleukin 4. We did phagocytosis and antigen presentation assays to investigate liver macrophages function as scavengers and immune response initiators. By using immunofluorescence staining, we further determined, in human liver tissue of patients with simple steatosis, non-alcoholic steatohepatitis, and chronic hepatitis B infection, the expression of the co-inhibitory protein CD274 (Programmed-death ligand 1) and major histocompatibility complex (MHC) class II.

Results: Both in humans and mice, within chronically inflamed fatty livers, liver macrophages acquired immunomodulatory properties by reducing the expression of MHC class II, and by enhancing co-inhibitory signalling. Liver macrophages circumscribed endotoxin-mediated inflammatory response by up-regulating anti-inflammatory genes arginase 1 and interleukin-10. While hepatic macrophages isolated from mice with normal livers were capable of achieving endotoxin tolerance, our results indicated an impairment of this protective mechanism in the presence NASH-like parenchymal abnormalities.

Conclusions: Liver macrophages can achieve endotoxin tolerance, but in the chronically-inflamed fatty liver, while they acquire an immunomodulatory phenotype, liver macrophages fail to dampen immune-mediated damage. Therefore, loss of tolerogenicity induced by ongoing liver insult may be a mechanism contributing to the worsening of NAFLD.

Abstract word-count: 248

KEYWORDS: Non-alcoholic fatty liver disease, non-alcoholic steatohepatitis, co-inhibition, programmed-death ligand 1, liver macrophages, PD-L1, endotoxin

LAY SUMMARY

This study indicates that liver macrophages respond to chronic tissue injury by limiting inflammation, but that non-alcoholic steatohepatitis (a pathological condition where lipids pathologically accumulate in the liver in the absence of alcohol intake) hinders this protective cell function.

INTRODUCTION

Non-alcoholic fatty liver disease (NAFLD) is the most common form of chronic liver disease in high-income countries, and it encompasses several stages of disease severity, which includes simple liver triglyceride accumulation (steatosis), steatosis with inflammation (non-alcoholic steatohepatitis [NASH]), liver fibrosis, and at the end of the spectrum, liver cirrhosis [1]. Although simple liver steatosis does not usually have clinically-meaningful consequences, evidence indicates that 25% [2] of patients with liver steatosis develop NASH, and that 25% of them progress to more advanced stages of severe fibrosis and liver cirrhosis [3].

NAFLD pathogenesis has often been interpreted within the "multiple-hits" paradigm, where hepatocellular lipid accumulation represents the "first hit", followed by several "second hits" resulting in further worsening of lipid accumulation, inflammation and tissue remodelling [4]. Liver macrophages are a key component to the second hits, given their unique location within the liver sinusoid, their capacity to clear pathogens circulating in the portal blood, and their ability to recruit circulating inflammatory cells [5].

On the other hand, intrahepatic scavenger cells are cornerstones to the maintenance of liver immune tolerogenicity, a process whereby chronic induction of immunity is constrained to avoid exaggerated immune-mediated liver damage, or even unnecessary activation against innocuous antigens [6,7]. While there is evidence that B7-mediated co-inhibitory signals dampen liver damage in situations such as ischemia-reperfusion injury [8] and chronic hepatitis B/C virus infection [9,10], less information exists on the relevance of immune tolerogenicity and on the function of liver macrophages in containing potentially harmful immune activation in the setting of worsening NAFLD.

In this study, using a novel isolation procedure, we assessed liver macrophages immune functions in a mouse model of NASH, specifically looking at liver macrophages inflammatory properties, phagocytic capacity, antigen presentation and co-stimulatory activity.

METHODS

Animals and models of chronic liver injury. All animal procedures were carried out under the terms of an experimental protocol approved by the ethical committee of the University of Geneva and by the Geneva veterinary authorities (GE 22/13). Eight-10 weeks old male C57Bl/6j mice were purchased from Janvier (Le Genest-Saint-Isle, France) and were housed under 12/12-hour light/dark cycles, with free access to food and water. For antigen presentation experiments, we used male OT-II mice from Charles River (C57BL/6-Tg(TcraTcrb)425Cbn/Crl). For the NASH-like liver injury model, liver steatosis was induced by feeding mice for 12 weeks with a choline-deficient diet, purchased from Kliba-Nafag (Kaiseraugst, Switzerland). This diet contains 15% of caloric content as crude fat and is supplemented in methionine. Choline-deficient diet was given for 12 weeks in order to induce significant hepatocellular lipid accumulation and hepatic inflammatory changes, based on our previous study [11]. Control animals received standard chow for the same duration. For some experiments, we used a model of chronic liver injury based on the administration of carbon tetrachloride (CCL4) [12]. In this model, mice receive a bi-weekly subcutaneous injection of CCL4 (0.5ul per gram of animal weight) for 6 weeks. Under this protocol, mice display failure to thrive and liver inflammation (supplementary Figure S1).

Human samples. Patients with morbid obesity and undergoing Roux-en-Y gastric bypass were prospectively recruited at Geneva University Hospitals, Switzerland. Liver biopsies were obtained during surgery. Twenty nine patients with healthy liver (n=10), simple steatosis without lobular inflammation (n=9) and histological NASH features (n=10) (as determined by the steatosis, activity and fibrosis (SAF) score) [13] were randomly selected for in depth analysis, after obtaining ethical approval by the local research ethics committee (protocol 14-125R). We further assessed liver biopsies of 10 patients with chronic hepatitis B virus infection (protocol 2017-084).

Liver paraffin sections (5µm) were dewaxed. Next, heat-mediated antigen retrieval (10mM citrate buffer, pH6 (MHC-II) or Tris-EDTA buffer, pH9 (PD-L1)) and saturation (Dako REAL Diluent supplemented with 2.5% Bovine Serum Albumin) were performed. Sections were incubated overnight with the following antibodies: mouse anti-human CD68 (clone PG M1, Dako) and rabbit anti-human class II MHC (EPR11226, RabMab) with Alexa-Fluor 555 donkey anti-mouse IgG (Invitrogen, Ref. A31570) and Alexa-Fluor 488 donkey anti-rabbit IgG (Jackson ImmunoResearch, Ref. 711-545-152) secondary antibodies. For PD-L1 staining, anti-CD68 antibody was incubated with rabbit anti-human CD274 (clone E1L3N, Cell Signalling) and the slides were then incubated with Atto 647 goat anti-mouse IgG3 secondary antibody (LS-C209483, LifeSpan Biosciences) and PD-L1 labelling was amplified with a TSA™ kit with Alexa-Fluor 568 (T20924, Themofischer Scientific). Nuclei were stained with Hoechst. Slides were

mounted and scanned with a Pannoramic 250 Flash II scanner (3DHISTECH Ltd, Budapest, Hungary) with resolution of 0.22 um/px. Images were analyzed using a custom rule-set using Definiens Developer XD (Definiens, Inc, Munich, Germany). Tissue detection was performed at a resolution of 4.4 um/px. Detection of $CD68^+$ cells and PD-L1 signal was performed using a random forest classifier at 0.44um/px. $CD68^+$ cells with at least 10% of PD-L1 co-staining were considered double positive. Finally, total tissue area and cell numbers were exported. The amount of MHC class II^+ signal within $CD68^+$ cells was quantified after rank-level background removal was performed for each marker channel.

Human gene expression and molecular pathway analysis.

We assessed the differential expression of molecular pathways of the co-stimulatory molecules *CD274*, *CD86* and *CD80* in the liver transcriptome of 73 subjects including 14 controls, 27 healthy obese, 14 NAFLD (simple steatosis without lobular inflammation) and 18 NASH subjects (GSE48452) [14]). Modulated molecular pathways in the NASH dataset were determined by applying relevant molecular pathway gene sets from the Molecular Signature Database (www.broadinstitute.org/msigdb) using Gene Set Enrichment Analysis (GSEA) [15]. Differentially expressed genes were expressed as fold change compared to control subjects.

Liver macrophages isolation and in vitro stimulation. Mice were anesthetized with inhaled isoflurane. Xypho-pubic laparotomy was performed, and mice were exsanguinated by venous puncture. The right atrium was exposed by thoracotomy, the supra-hepatic inferior vena cava was cannulated, and the liver was perfused in a retrograde fashion with a wash solution (HBSS, EGTA 0.5 mM, HEPES 25 mM, Penicillin-Streptomycin 1 μg/ml, Glucose 0.1% and Heparin 5 U/ml). Next, liver digestion was performed for five minutes (5 ml/min, 37°C, IMDM, Collagenase IV, Worthington at 0.5mg/ml, and DNAse I, Roche at 0.1mg/ml). Digested livers were filtered on a 70 μm nylon cell strainer. Hepatocytes were discarded after two 5-min centrifugations at 68g, 4°C. Liver macrophages-rich fraction was obtained by density gradient centrifugation (1400g, no acceleration nor brake) on OptiPrep 17.4%-8.2% (Sigma). Cells at the interface were washed twice, and positive selection was performed by magnetic cell sorting using CD11b-coupled microbeads and LS MACS columns (Miltenyi Biotech). Using this isolation procedure, highly purified (>95%) populations of Clec4-positive liver macrophages were obtained. Liver macrophages were cultured in Roswell park institute medium (RPMI) supplemented with 10% fetal calf serum (FCS). For some experiments, liver macrophages were stimulated with lipopolysaccharide (LPS, 2 μg/ml, Sigma) or interleukin 4 (IL-4, 5 ng/ml, R&D systems), respectively. After 24h hours of exposition to LPS or IL-4, supernatant was collected, whole cell

lysates were obtained by using Trizol reagent (Ambion), and total RNA was extracted using the RNeasy Mini Kit (Qiagen).

Liver macrophages phagocytosis. Liver macrophages phagocytosis was assessed both by confocal microscopy and by FACS analysis. Briefly, $3x10^4$ isolated liver macrophages were seeded on a coverglass in a 24w plate and were allowed to adhere for 30 min. Next, $2.5x10^5$ mouse B-cell lymphoma (YAC) cells stained with DiI (ThermoFischer Scientific) were seeded in the wells. After 45min, wells were washed vigorously to remove non-internalized YAC cells. Liver macrophages were stained with a rat anti-mouse F4-80 antibody (clone CI-A3:1, Bio-Rad), counterstained with an Alexa-488 chicken anti-rat secondary antibody and fixed with 4% paraformaldehyde. Nuclei were stained with Hoechst. Images were taken with a LSM 510-meta confocal microscope (Zeiss). For *in vivo* phagocytosis assay, DiI-labelled YAC cells were injected in the portal vein. After 30 or 120 min, we isolated liver macrophages as described above, and we did FACS analysis to determine the ratio of double-positive F4-80$^+$/DiI cells to total F4-80$^+$ cells.

Antigen-presentation assay. Antigen presentation was tested both *in vitro* and *in vivo*. To assess the capacity of liver macrophages (retrieved from steatotic livers, or CCL4-injured livers *vs*. control livers) to act as antigen-presenting cells, ovalbumin-specific CD4$^+$ T cells were isolated from the peripheral lymphoid organs of OT-II mice by negative sorting using a CD4$^+$ T cell isolation kit (Miltenyi Biotech) and stained with carboxyfluorescein succinimidyl ester (CFSE, 0.5μM). One hundred thousand liver macrophages from steatotic, CCL4-injured, and control mice were isolated as described above, and were allowed to process the ovalbumin-peptide (OVA 323-339) for 3h. After vigorous washing to remove the peptide-containing supernatant, CFSE-labelled ovalbumin-specific CD4$^+$ T cells were added to the wells in a 1:5 ratio, and co-cultured with liver macrophages for 48h (*in vitro* assessment). For *in vivo* antigen presentation assessment, peptide-loaded liver macrophages were detached, and re-injected along with CFSE-labelled ovalbumin-specific CD4$^+$ T cells in the portal vein of wild type mice. After 48h, we isolated mononuclear cells from lymphoid organs and liver. As a measure of the capacity of our liver macrophages to present antigens, we did FACS analysis to determine the number of proliferating (CFSE^{low}) and non-proliferating (CFSE^{high}) CD4$^+$ T cells.

Flow cytometry analysis (FACS). Liver macrophages were characterized by FACS analysis. Cells were incubated with Fc-blocking reagent (TrueStain, Biolegend) for 5 min, and stained for 20min at 4°C with appropriate antibodies from Biolegend: FITC anti-F4-80 (BM8), APC anti-I-A-I-E (M5/114.15.2), PE anti-CD86 (GL-1), PECy7 anti-CD68 (FA-11), PerCP anti-CD11b (M1/70) and

PE anti-B7-homolog 1 (also known as programmed-death ligand 1 [PD-L1] or CD274, MIH5) (eBioscience). Samples were acquired with a Flow Cytometer Cyan (Beckman Coulter) and analyzed with FloJo (Treestar). Results of FACS analysis are presented as the median of the mean *fluorescence index (MFI)* (± interquartile range).

Real-time polymerase chain reaction (qPCR). After total RNA (cells or liver tissue) extraction, one μg of cDNA was synthesized by extending a mix of random primers with the High Capacity cDNA Reverse Transcription Kit in the presence of RNAase Inhibitor (Applied Biosystems). The relative quantity of each transcript was normalized to the expression of ribosomal protein large P1 (*Rplp1*). Amplification were carried out in a total volume of 20 μl using a thermocycler sequence detector (BioRad CFX96) with qPCR Core kit for SYBR Green I (Eurogentec). Primer sequences used in the present study are available upon request.

Statistical analysis. Statistical analyses were computed using Prism 6 (GraphPad Software Inc., La Jolla, California, US). Data are expressed as median ± interquartile range of at least three independent experiments and were compared using the non-parametric tests unless otherwise specified. Bioinformatics analyses were performed using the R statistical language (www.r-project.org).

RESULTS

Exploratory analysis of the immune phenotype in the human fatty liver.

To explore the immune phenotype in human NAFLD, we first did computational analyses based on a publicly available dataset (GSE48452), and measured, within livers of patients with increasingly severe NAFLD lesions, the relative expression of genes encoding the immune co-stimulatory/inhibitory molecules CD80, CD86 and CD274. Results indicated that livers with increasingly severe lesions displayed significantly higher expression of the co-stimulatory proteins CD86 and CD80, and lower expression of the co-inhibitory protein CD274 (Figure 1A). Looking at the functional translation of this phenotype, we analysed molecular pathways downstream of the various receptors binding CD80, CD86 and CD274, that is CD28, CTLA-4 and PD-1. Gene set enrichment analysis revealed that, as compared to less severe stages of fatty liver disease, livers with NASH displayed increased activation of these three receptors (Figure 1B). Results further indicated that there was a marked activation of dendritic cells and macrophages, with the latter harbouring an M2-like phenotype (Figure 1B). Of note, these analyses are run on whole liver tissue, and do not specifically assess gene expression and molecular pathways on liver resident macrophages (patients with NAFLD have more infiltrating immune cells). Therefore, we sought to further characterize liver macrophages phenotype and function in a mouse model of diet-induced NASH.

Liver macrophages inflammatory phenotype in chronic, diet-induced steatohepatitis.

After 12 weeks of feeding on a choline-deficient diet, mouse livers were enlarged and showed yellowish discoloration, consistent with our previous observations that choline-deficient diet elicits steatohepatitis [11]. We isolated liver macrophages from mouse livers with or without diet-induced steatohepatitis, by *in vivo* liver perfusion, non-parenchymal cell isolation and magnetic cell sorting. As previously described [16], a specific flow cytometry-labelling strategy assessed the purity of the liver macrophages population. The isolated population expressed Clec4, a marker of Kupffer cells in mice, but did not express Ly6C, which is only expressed on bone-marrow derived passenger macrophages. Of note, the isolated population included, on average, 2.3% (±1.54) of F4-80^{low} cells which did not express Clec4 (supplementary Figure 2).

Liver macrophages were assessed for their susceptibility to get polarized into M1 or M2 macrophages, after a 24h challenge with LPS or IL-4 (Figure 2). While IL-4 treatment did not result in pronounced differences between study groups, LPS challenge elicited a significantly greater upregulation in the expression of pro-inflammatory genes *Mcp-1* and *iNos* in liver macrophages from NASH livers as compared to their lean counterparts. Similar to other data [17,18],

Arg-1 (P=0.016) expression was also elevated after 24h of exposition to LPS, suggesting negative feedback loops restricting the intensity of liver macrophages response to LPS stimulation [19], particularly in NASH livers (Figure 2). We further performed qPCR analysis for the same genes on liver macrophages harvested from mouse livers submitted to CCL4 liver injury. Using this model, upon LPS challenge, the expression *iNos*, but not that of *Mcp-1* or *Arg-1*, was significantly different between CCL4-treated and control animals (supplementary Figure S3).

Liver macrophages phagocytosis is not impaired by diet-induced steatohepatitis.

Beyond overly archetypal M1-M2 dichotomy, we reasoned that alterations in the level of expression of *iNos* (*Nos2*) and *Arg-1* may reflect changes in liver macrophages function in a chronic, NASH-like inflammatory context [20,21]. Therefore, we assessed primary liver macrophage phagocytosis function, using several approaches. First, freshly isolated liver macrophages were exposed to DiI-labelled syngeneic mouse B cell lymphoma (YAC) cells. Thereafter, we did confocal microscopy (Figure 3A) and FACS analysis (Figure 3B) to determine the proportion of liver macrophages that had internalized YAC cells. These two experiments yielded similar findings in that primary liver macrophages are potent phagocytosis effectors (with 40-50% of them showing evidence of YAC cell internalization), and that the presence of NASH did not alter this function. We further assessed liver macrophages phagocytosis in vivo. Via portal vein puncture, we injected YAC^{DiI} into mouse livers. After 30 or 120 min, we isolated liver macrophages, and determined the percentage of these cells that had internalized DiI-labelled YAC cells, by FACS analysis. Results consistently indicated that the scavenger function of liver macrophages was not affected in our diet-induced liver steatohepatitis model (Figure 3C).

Impairment of liver macrophages-mediated immune tolerogenicity in chronically inflamed NASH livers.

Given the pivotal role of non-parenchymal cells in the maintenance of immune tolerogenicity [22-24], we sought to assess the contribution of liver macrophages to the modulation of immune activation, both in the presence of NASH-like and CCL4-induced chronic liver injury . To do so, we measured by FACS analysis the expression levels of molecules conveying cell-cell interactions during immune responses, such as class II major histocompatibility complex (class II MHC), co-inhibitory CD274 (PD-L1) and co-stimulatory CD86. Results indicated that class II MHC was significantly down-regulated in both models of liver injury (Figure 4A). In contrast co-inhibitory molecule PD-L1 was noticeably upregulated only on liver macrophages isolated from NASH livers (Figure 4B). Both in the CCL4 and diet-induded NASH models, the expression of CD86 was not altered (Figure 4C). These findings suggest that in the presence of chronic liver

injury, and even more so with NASH-like lesions, liver macrophages acquire a tolerogenic phenotype in order to dampen harmful immune activation [25].

To further investigate whether such a tolerogenic phenotype would translate into functional alterations, we analysed liver macrophages capacity to present antigens to $CD4^+$ T cells. Antigen presentation assays were first performed on liver macrophages procured from mouse livers without parenchymal alterations, and in the presence of LPS (or not). After endotoxin challenge, consistent with other data [6] and with our observation of both an increased IL-10 expression (Figure 5A) and a decreased surface class II MHC expression (Figure 5B), we found that the efficacy of liver macrophages at presenting antigens to $CD4^+$ T cells was reduced upon endotoxin exposure (Figure 5C), a process known as endotoxin tolerance, or PAMP hypo-responsiveness [6,26]. We next sought to determine whether chronic liver injury, such as that provoked by diet-induced NASH or CCL4 administration, jeopardized liver macrophages maintenance of tolerogenicity. For this purpose, we did additional antigen presentation assays, comparing antigen presentation capacity by liver macrophages from control vs. chronically injured livers, in the presence or absence of endotoxin stimulation. Results indicated that, as opposed to the control condition, within NASH livers, hepatic macrophage-mediated immune tolerogenicity was impaired, as evidenced by a capacity to process and present antigens to $CD4^+$ T cells similar to that of unstimulated counterparts (Figure 6A). *In vivo* experiments indicated a similar trend, but the difference did not reach significance (Figure 6B). We repeated the *in vitro* procedure using the CCL4-injury model, and found a similar impairment of endotoxin tolerance in the presence of chronic liver inflammation (Figure 6C).

Expression of class II MHC and CD274 on human liver macrophages in patients with increasingly severe NASH lesions and chronic hepatitis B virus infection.

We finally analysed 29 liver specimens procured from liver biopsy performed during Roux-en-Y gastric bypass surgery (Table 1). Consistent with the above results, there was a gradual decrease in the expression of class II MHC in hepatic macrophages from patients with control livers, those with liver steatosis without inflammation, and those with NASH lesions (as characterized by the presence of hepatocellular ballooning and lobular inflammation) (Figure 7A). While CD274 was not detected on liver macrophages from control livers, we measured an increase in the expression of this co-inhibitory molecule on liver macrophages from patients with simple steatosis, and NASH lesion (Figure 7B). In an effort to understand whether these observed features are specific to patients with NASH, we further analyzed 10 distinct liver biopsies procured from patients with chronic hepatitis B infection (supplementary Table 1), and compared them to the biopsies of the 10 control patients. In these non-NASH patients, class II MHC was similar between groups, and there was a trend towards increased PD-L1 expression in patients with chronic hepatitis B (supplementary Figure S4). Note that, in contrast to what was observed in mice, CD274 was expressed on a limited number of human liver macrophage.

DISCUSSION

Here, we show that in chronic liver injury, liver macrophage immune-signalling machinery is altered. While primary liver macrophages isolated from normal mouse livers were capable of mitigating endotoxin-mediated immune activation, our results suggest an exhaustion of such protective mechanisms in the presence of chronic liver inflammation. qPCR analysis revealed increased expression of both *iNos* and *Arg-1*, two enzymes that compete for their substrate, arginine, and that are pivotal in shaping macrophage function. For instance, after penetrating the phagosome, iNos-produced nitric oxide (NO) combines with superoxide to form peroxynitrite, which serves as potent antimicrobial product [27]. Moreover, elevated iNos and arginase levels may indicate sustained antigen presentation by liver macrophages, given that $CD4^+$ helper T cells 1 characteristically produce interferon γ, which can strongly activate macrophages to upregulate *iNos* expression [28].

Growing evidence supports that in the chronically inflamed liver, negative co-stimulation mediated by B7 family members confers protection to the liver against unnecessary or excessive immune damage [29]. Using immunohistochemistry staining of human liver biopsies (n=74), Kessel et al. have shown that chronically inflamed livers display increased expression of PD1 and its ligands PD-L1 and CD273 [25]. In the specific context of NAFLD, Chatzigeorgiou and colleagues reported that mice with genetic inactivation of both CD80 and CD86 develop worsened obesity-related metabolic dysregulation, glucose intolerance, and enhanced progression to steatohepatitis [30]. Our study reports a 50% elevation in co-inhibitory PD-L1 expression in liver macrophages isolated from the fatty -as compared to lean- mouse livers. Of note, when using a model of chemically-induced, non-NASH liver injury (CCL4), such a difference was observed. We found no difference in terms of CD86 expression, which can act as ligand for both the stimulatory CD28 receptor and the inhibitory CD152 (CTLA-4) inhibitory receptor on T cells [29]. Therefore, the role of CD86 expression, as well as other unassessed molecules involved in co-stimulation, remains to be further investigated. Thus far, our results suggest that in the presence of a NASH-like liver injury, liver macrophages expression of co-stimulatory molecules is shifted towards inhibitory signals. Immunostaining of human livers with increasingly severe NAFLD/NASH lesions supported the latter statement, as evidenced by a decrease in class II MHC expression and an increase in PD-L1 expression. Of note, the expression of these two proteins was not significantly different between control patients and those diagnosed with chronic hepatitis B virus infection.

By exemplifying the paradigm of endotoxin tolerance [6], our study highlights how hepatic non-parenchymal cells, such as liver macrophages, are unique in assisting the liver to circumscribe exaggerated immune activation, while maintaining efficient phagocytosis to clear portal blood

from toxic products. There is a remarkable heterogeneity in the subsets of macrophages populating the liver and differences between circulating and resident macrophages are important to consider when studying liver disease. Most resident Kupffer cells derive from yolk sac and/or from fetal liver progenitor cells, and the pool of Kupffer cells is maintained by self-renewal, independently from hematopoiesis [31,32]. Kupffer cells are radioresistant, long-lived, and are present in the liver both under steady-state and inflammatory conditions [32], whereas circulating bone marrow-derived monocytes, that express high levels of Ly6C [33], undergo recruitment and clearance depending on the balance of signals promoting or circumscribing inflammation, respectively [34]. Moreover, given their privileged microanatomical location in the liver sinusoid (mainly in the periportal area), Kupffer cells are at the forefront of the pathogenesis of diet-induced NASH, where toxic antigens, dietary lipids, bacterial wall components and cell debris reach the liver via the portal circulation. In this regard, a strength of this study is that it provides findings based on a >95% Clec4-positive population of liver macrophages, that one may consider to be Kupffer cells. But on the other hand, during chronic liver injury, circulating monocytes undergo recruitment and activation in the damaged liver [32], and participate in the pathogenesis of chronic liver disease. One could therefore object that the contribution of infiltrating macrophages is lacking to our study. In this regard, using an *in vivo* model of particle-bound antigen administration, Heymann et al. have shown that the maintenance of a tolerogenic liver environment is dependent on resident Kupffer cells rather than infiltrating bone-marrow derived monocytes [7].

There are limitations to our study. First, while we have looked at how diet-induced NASH alters liver macrophage function at dampening immune response, our study does not provide clinically-relevant information on how our results may translate to patient care. In this regard, one could consider that bacterial defense and/or tumor surveillance could be impacted by altered macrophage responses, a speculation that is particularly relevant to the NASH context, where patients are more prone to infection, and to the development of hepatocellular carcinoma. Second, our study did not examine other factors such as intracellular trafficking of MHC and co-stimulatory molecules [35,36]. To this end, Veglia and colleagues have recently shown that lipid bodies accumulation within cancer-associated dendritic cells hinders MHC trafficking from the phagosome/lysosome to the cell surface, thereby jeopardizing dendritic cells capacity at stimulating antigen-specific T cells expansion [37]. Finally, the use of a diet-induced model of NASH could be criticized as it may not fully recapitulate the precise pathophysiology of human NASH.

Collectively, our results indicate that, in the normal liver, primary liver macrophages can achieve endotoxin tolerance by upregulating expression of anti-inflammatory genes, and by displaying reduced antigen presentation capacity. In the chronically-inflamed fatty liver, despite the acquisition of immunomodulatory phenotype, liver macrophages have a reduced efficacy at dampening immune-mediated damage. Therefore, loss of tolerogenicity induced by ongoing liver insult may be a mechanism contributing to the worsening of NAFLD.

1. Michelotti GA, Machado MV, Diehl AM. NAFLD, NASH and liver cancer. Nat Rev Gastroenterol Hepatol. 2013;10:656-665.
2. Clark JM, Brancati FL, Diehl AM. The prevalence and etiology of elevated aminotransferase levels in the United States. Am J Gastroenterol. 2003;98:960-967.
3. McCullough AJ. The clinical features, diagnosis and natural history of nonalcoholic fatty liver disease. Clin Liver Dis. 2004;8:521-533, viii.
4. Jou J, Choi SS, Diehl AM. Mechanisms of disease progression in nonalcoholic fatty liver disease. Semin Liver Dis. 2008;28:370-379.
5. Baffy G. Kupffer cells in non-alcoholic fatty liver disease: the emerging view. J Hepatol. 2009;51:212-223.
6. Thomson AW, Knolle PA. Antigen-presenting cell function in the tolerogenic liver environment. Nat Rev Immunol. 2010;10:753-766.
7. Heymann F, Peusquens J, Ludwig-Portugall I, et al. Liver inflammation abrogates immunological tolerance induced by Kupffer cells. Hepatology. 2015;62:279-291.
8. Ji H, Shen X, Gao F, et al. Programmed death-1/B7-H1 negative costimulation protects mouse liver against ischemia and reperfusion injury. Hepatology. 2010;52:1380-1389.
9. Jeong HY, Lee YJ, Seo SK, et al. Blocking of monocyte-associated B7-H1 (CD274) enhances HCV-specific T cell immunity in chronic hepatitis C infection. J Leukoc Biol. 2008;83:755-764.
10. Chen L, Zhang Z, Chen W, et al. B7-H1 up-regulation on myeloid dendritic cells significantly suppresses T cell immune function in patients with chronic hepatitis B. J Immunol. 2007;178:6634-6641.
11. Orci LA, Berney T, Majno PE, et al. Donor characteristics and risk of hepatocellular carcinoma recurrence after liver transplantation. Br J Surg. 2015;102:1250-1257.
12. Dong S, Chen QL, Song YN, et al. Mechanisms of CCl4-induced liver fibrosis with combined transcriptomic and proteomic analysis. J Toxicol Sci. 2016;41:561-572.

13. Bedossa P, Consortium FP. Utility and appropriateness of the fatty liver inhibition of progression (FLIP) algorithm and steatosis, activity, and fibrosis (SAF) score in the evaluation of biopsies of nonalcoholic fatty liver disease. Hepatology. 2014;60:565-575.
14. Ahrens M, Ammerpohl O, von Schonfels W, et al. DNA methylation analysis in nonalcoholic fatty liver disease suggests distinct disease-specific and remodeling signatures after bariatric surgery. Cell Metab. 2013;18:296-302.
15. Subramanian A, Tamayo P, Mootha VK, et al. Gene set enrichment analysis: a knowledge-based approach for interpreting genome-wide expression profiles. Proc Natl Acad Sci U S A. 2005;102:15545-15550.
16. Lacotte S, Slits F, Orci LA, et al. Impact of myeloid-derived suppressor cell on Kupffer cells from mouse livers with hepatocellular carcinoma. Oncoimmunology. 2016;5:e1234565.
17. Bronte V, Serafini P, De Santo C, et al. IL-4-induced arginase 1 suppresses alloreactive T cells in tumor-bearing mice. J Immunol. 2003;170:270-278.
18. Sonoki T, Nagasaki A, Gotoh T, et al. Coinduction of nitric-oxide synthase and arginase I in cultured rat peritoneal macrophages and rat tissues in vivo by lipopolysaccharide. J Biol Chem. 1997;272:3689-3693.
19. Knolle P, Schlaak J, Uhrig A, Kempf P, Meyer zum Buschenfelde KH, Gerken G. Human Kupffer cells secrete IL-10 in response to lipopolysaccharide (LPS) challenge. J Hepatol. 1995;22:226-229.
20. Billiar TR, Curran RD, Stuehr DJ, West MA, Bentz BG, Simmons RL. An L-arginine-dependent mechanism mediates Kupffer cell inhibition of hepatocyte protein synthesis in vitro. J Exp Med. 1989;169:1467-1472.
21. Navarro LA, Wree A, Povero D, et al. Arginase 2 deficiency results in spontaneous steatohepatitis: a novel link between innate immune activation and hepatic de novo lipogenesis. J Hepatol. 2015;62:412-420.
22. Mazzoni A, Bronte V, Visintin A, et al. Myeloid suppressor lines inhibit T cell responses by an NO-dependent mechanism. J Immunol. 2002;168:689-695.
23. Muller AJ, Scherle PA. Targeting the mechanisms of tumoral immune tolerance with small-molecule inhibitors. Nat Rev Cancer. 2006;6:613-625.

24. Munder M. Arginase: an emerging key player in the mammalian immune system. Br J Pharmacol. 2009;158:638-651.
25. Kassel R, Cruise MW, Iezzoni JC, Taylor NA, Pruett TL, Hahn YS. Chronically inflamed livers up-regulate expression of inhibitory B7 family members. Hepatology. 2009;50:1625-1637.
26. Biswas SK, Lopez-Collazo E. Endotoxin tolerance: new mechanisms, molecules and clinical significance. Trends Immunol. 2009;30:475-487.
27. Pryor WA, Squadrito GL. The chemistry of peroxynitrite: a product from the reaction of nitric oxide with superoxide. Am J Physiol. 1995;268:L699-722.
28. Niedbala W, Cai B, Liew FY. Role of nitric oxide in the regulation of T cell functions. Ann Rheum Dis. 2006;65 Suppl 3:iii37-40.
29. Corse E, Gottschalk RA, Park JS, et al. Cutting edge: chronic inflammatory liver disease in mice expressing a CD28-specific ligand. J Immunol. 2013;190:526-530.
30. Chatzigeorgiou A, Chung KJ, Garcia-Martin R, et al. Dual role of B7 costimulation in obesity-related nonalcoholic steatohepatitis and metabolic dysregulation. Hepatology. 2014;60:1196-1210.
31. Yona S, Kim KW, Wolf Y, et al. Fate mapping reveals origins and dynamics of monocytes and tissue macrophages under homeostasis. Immunity. 2013;38:79-91.
32. Zigmond E, Samia-Grinberg S, Pasmanik-Chor M, et al. Infiltrating monocyte-derived macrophages and resident kupffer cells display different ontogeny and functions in acute liver injury. J Immunol. 2014;193:344-353.
33. Ramachandran P, Pellicoro A, Vernon MA, et al. Differential Ly-6C expression identifies the recruited macrophage phenotype, which orchestrates the regression of murine liver fibrosis. Proc Natl Acad Sci U S A. 2012;109:E3186-3195.
34. Holt MP, Cheng L, Ju C. Identification and characterization of infiltrating macrophages in acetaminophen-induced liver injury. J Leukoc Biol. 2008;84:1410-1421.
35. Chow A, Toomre D, Garrett W, Mellman I. Dendritic cell maturation triggers retrograde MHC class II transport from lysosomes to the plasma membrane. Nature. 2002;418:988-994.

36. Turley SJ, Inaba K, Garrett WS, et al. Transport of peptide-MHC class II complexes in developing dendritic cells. Science. 2000;288:522-527.
37. Veglia F, Tyurin VA, Mohammadyani D, et al. Lipid bodies containing oxidatively truncated lipids block antigen cross-presentation by dendritic cells in cancer. Nat Commun. 2017;8:2122.

Table 1 Clinical characteristics of the included patients.

	Control	NAFLD	NASH
n	10	9	10
Age	41 (38-46)	35 (30-47)	44 (38-51)
Female (%)	80	67	70
BMI (kg/m^2)	37 (37-37)	41.5 (40.4-53)	43.6 (41-46)
ALT (iU/l)	24 (19-32)	44 (20-88)	35 (27-70)
Type II diabetes (y:n)	1:9	2:7	4:6
Fibrosis value	0 (0-0)	0 (0-0)	1.5 (1-2)
SAF score	0 (0-1)	3 (2-4)	7 (6-7)

Values are median (interquartile range) unless otherwise specified. Non-alcoholic fatty liver disease (NAFLD), Non-alcoholic steatohepatitis (NASH), Steatosis-Activity-Fibrosis (SAF)

Figure legends.

Figure 1. Exploratory analysis of the immune phenotype in the human fatty liver. Data from the publicly available dataset GSE48452 were accessed, and the relative expression of genes encoding the immune co-stimulatory/inhibitory molecules *CD80*, *CD86* and *CD274 (PD-L1)* was quantified. On top of the heatmap, a coloured legend indicates relative fold change expression compared to control livers (**A**). Gene set enrichment analysis on whole liver tissue explore cell signalling downstream to the designed pathways. On top of the heatmap, a coloured legend indicates relative molecular pathway induction compared to control livers (**B**).

Figure 2. Differential gene expression of primary liver macrophages isolated from control versus NASH-like livers. Isolated liver macrophages were exposed to lipopolysaccharide (1 ug/ml) or interleukin 4 (100 ng/ml) and expression of pro-inflammatory M1 markers genes (macrophage chemoattractive protein 1 [*Mcp-1*] (**A**), inducible nitric oxide synthase [*Nos2*] (**B**)) and anti-inflammatory M2 markers genes (arginase 1 [*Arg1*] (**C**), *Il10* (**D**), *Cd206* (**E**) and *Cd163* (**F**) were measured by qPCR. The relative quantity of each transcript was normalized to the

expression of the housekeeping gene *Rplp1* and expressed as fold change relative to the negative-control condition. Data represent median and interquartile range.

Figure 3. Diet-induced NASH does not alter liver macrophages phagocytosis capacity (continued). Confocal microscopy and quantification of phagocytosis of YAC cells by liver macrophages isolated from control livers, or livers with diet-induced NASH. YAC cells are labelled in red with DiI, and liver macrophages are labelled in green with an FITC-conjugated anti-F4-80 antibody. At least three fields per sample were analysed (**A**). *In vitro* (**B**) and *in vivo* (**C**) FACS analysis of liver macrophages phagocytosis. Inserts show one representative experiment. Data represent median and interquartile range.

Figure 4. Membranous expression of class II MHC and co-inhibitory PD-L1 expression on liver macrophages in NASH-like and carbon tetrachloride (CCL4)-induced models of liver injury. (A) Class II major histocompatibility complex (MHC) was significantly less expressed on liver macrophages from mice with both diet-induced NASH (left) and CCL4 liver injury (right), as compared to control. **(B)** Similar expression of the co-stimulatory molecule CD86 across studied conditions (diet-induced NASH, CCL4 injury, left and right respectively). The co-inhibitory molecule CD274 (Programmed-death ligand 1, PD-L1) was significantly more expressed only on liver macrophages isolated from livers with NASH lesions (left panel), but not in the CCL4 model (right panel). Inserts show results from one representative experiment. Data show median and interquartile range.

Figure 5. Endotoxin tolerance in primary liver macrophages. Lipopolysaccharide-challenged primary liver macrophages display a significantly higher cell expression of IL-10 (**A**), significantly lower membranous expression of class II MHC (**B**), and reduced antigen presentation capacity (**C**). Data represent median and interquartile range of five independent experiments.

Figure 6. Impairment of immune tolerogenicity in chronic liver injury. (**A**) *in vitro* and (**B**) *in vivo* antigen presentation assays in livers with or without diet-induced NASH lesions. (C) Antigen presentation assay in livers with or without CCL4-injury. Data represent median and interquartile range.

Figure 7. Human liver macrophages in NASH patients display decreased expression of class II MHC and increased expression of PD-L1. Images illustrate the reduced abundance of double-positive $CD68^+$(red)/class II MHC^+(green) (left panels (A), yellow arrows) and the increased abundance of double-positive $CD68^+$(red)/PD-L1($CD274^+$, green) (right panels (B), yellow arrows) liver macrophages, in patients with increasingly severe NAFLD/NASH lesions. Scale bars, 50 μm (left panels) and 20μm (right pannels).

Appendices (Supplementary material)

Supplementary Figure S1. Chronic carbon tetrachloride (CCL4) administration as a model of liver injury. Mice were given for 6 weeks a bi-weekly injection of CCL4 to induce chronic liver inflammation. Under this protocol, mice displayed failure to thrive (left panel) and elevated blood level of alanine aminotransferase (right panel).

Supplementary Figure S2. Clec4 expression on isolated liver macrophages. After magnetic beads sorting, the vast majority of isolated cells are $Clec4^{+}$ and are therefore considered to be Kupffer cells. The remaining cell-subset (2.3% (±1.54) display a baseline Clec4 mean fluorescence intensity similar to that of other $F4\text{-}80^{low}$ cell subsets.

Supplementary Figure S3. Differential gene expression of primary liver macrophages isolated from control versus CCL4-injured liver. Isolated liver macrophages were exposed to lipopolysaccharide (1 ug/ml) or interleukin 4 (100 ng/ml) and expression of pro-inflammatory M1 markers genes (macrophage chemoattractive protein 1 [*Mcp-1*] (**A**), inducible nitric oxide synthase [*Nos2*] (**B**)) and anti-inflammatory M2 markers genes (arginase 1 [*Arg1*] (**C**), *Il10* (**D**), *Cd206* (**E**) and *Cd163* (**F**) were measured by qPCR. The relative quantity of each transcript was normalized to the expression of the housekeeping gene *Rplp1* and expressed as fold change relative to the negative-control condition. Data represent median and interquartile range.

Supplementary Figure S4. Human liver macrophages in patients with chronic hepatitis B virus infection do not display different expression of class II MHC and PD-L1. Data represent median and interquartile range of n=10 patients with chronic hepatitis B virus infection.

Figure 1

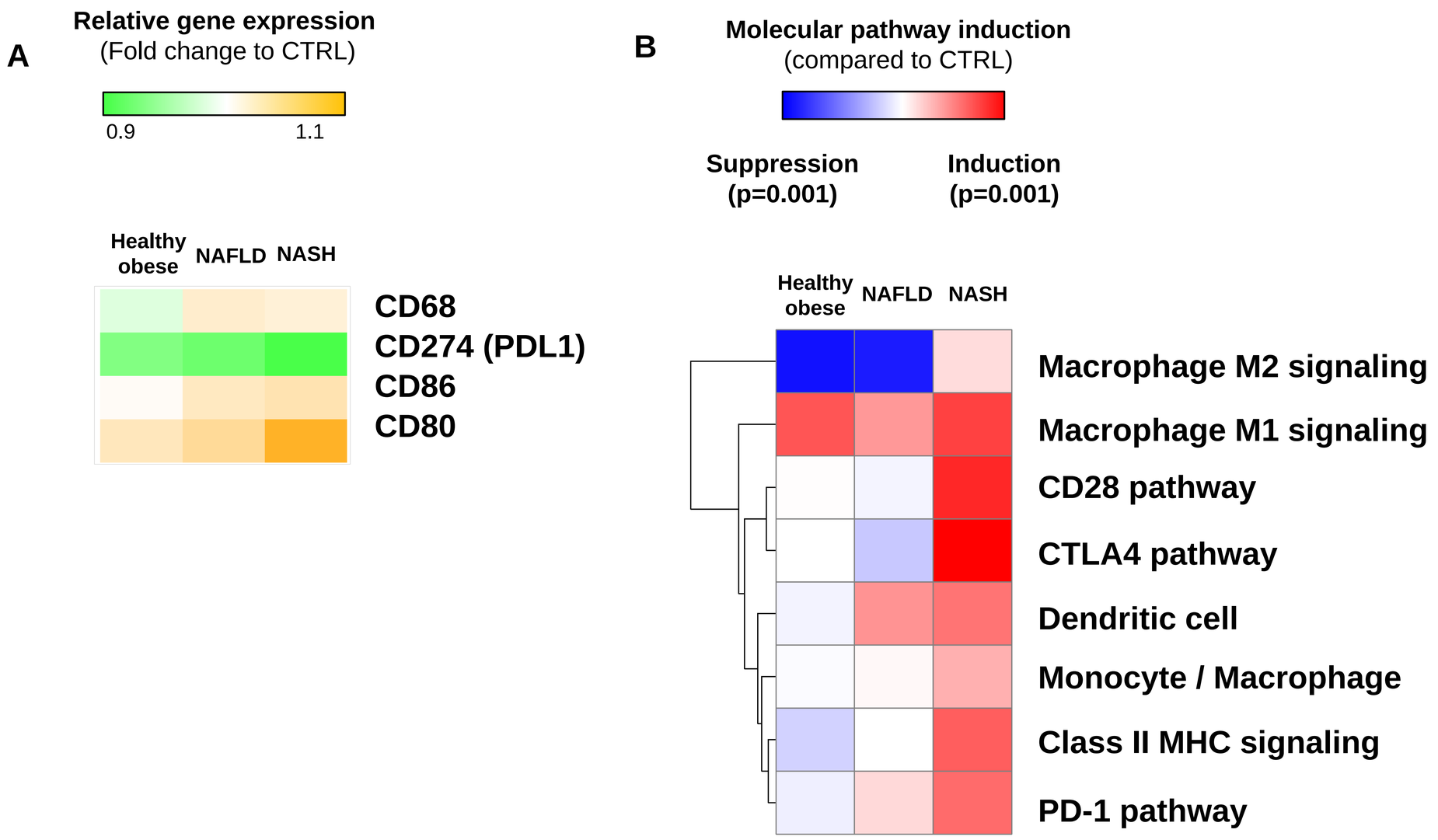
A
Relative gene expression
(Fold change to CTRL)
0.9
1.1
Healthy obese
NAFLD
NASH
CD68
CD274 (PDL1)
CD86
CD80
B
Molecular pathway induction
(compared to CTRL)
Suppression (p=0.001)
Induction (p=0.001)
Healthy obese
NAFLD
NASH
Macrophage M2 signaling
Macrophage M1 signaling
CD28 pathway
CTLA4 pathway
Dendritic cell
Monocyte / Macrophage
Class II MHC signaling
PD-1 pathway

Figure 2

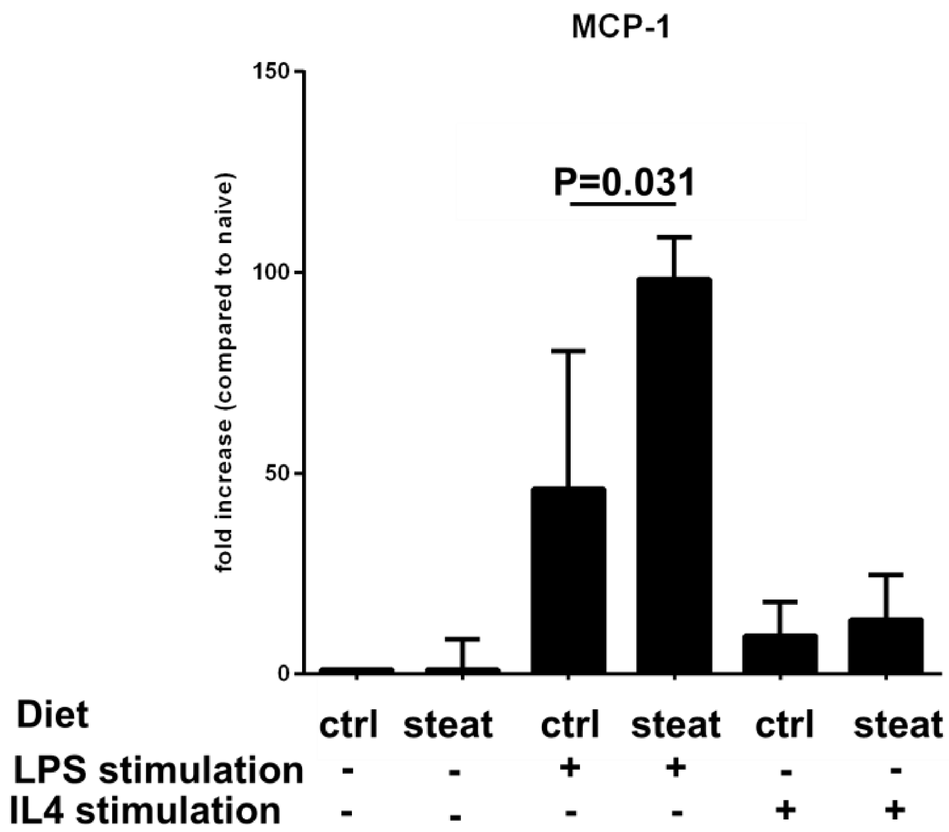
MCP-1
P=0.031
fold increase (compared to naive)
150
100
50
0
Diet
ctrl steat ctrl steat ctrl steat
LPS stimulation - - + + - -
IL4 stimulation - - - - + +

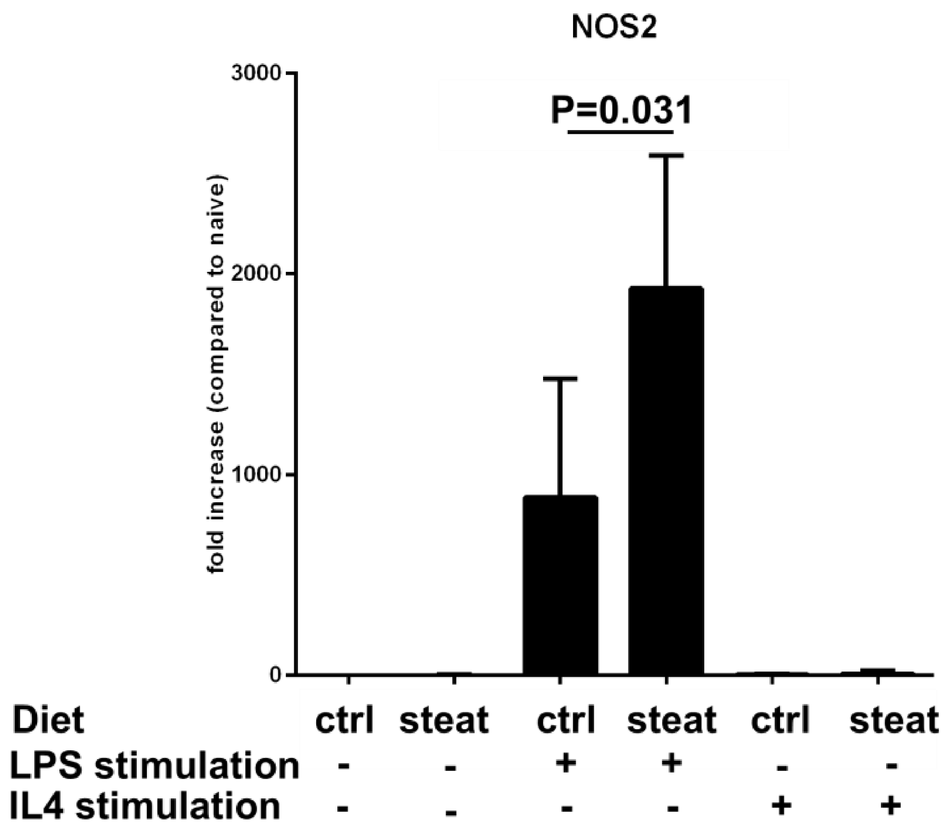
NOS2
P=0.031
fold increase (compared to naive)
3000
2000
1000
0
Diet
ctrl steat ctrl steat ctrl steat
LPS stimulation - - + + - -
IL4 stimulation - - - - + +

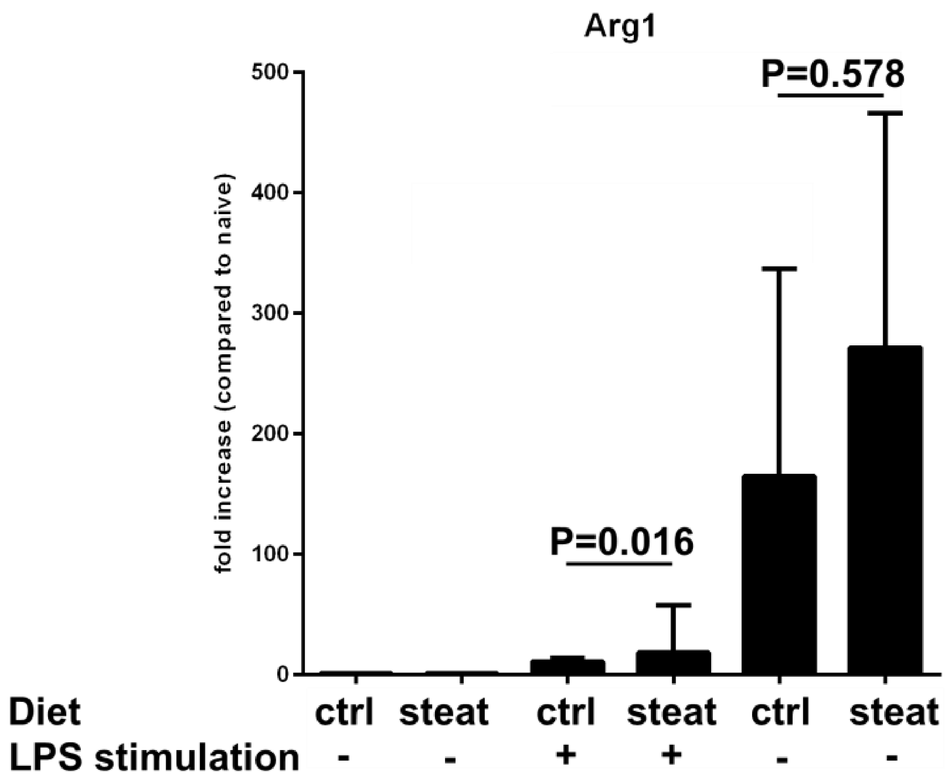
Arg1
P=0.578
P=0.016
fold increase (compared to naive)
500
400
300
200
100
0
Diet
ctrl steat ctrl steat ctrl steat
LPS stimulation - - + + - -
IL4 stimulation - - - - + +

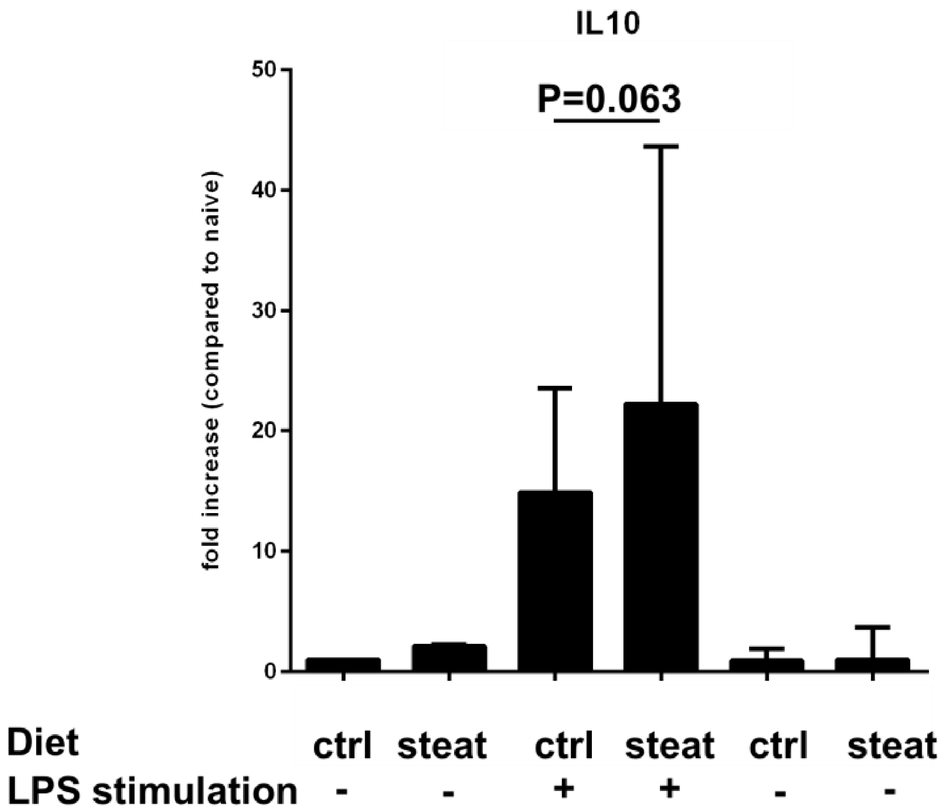
IL10
P=0.063
fold increase (compared to naive)
50
40
30
20
10
0
Diet
ctrl steat ctrl steat ctrl steat
LPS stimulation - - + + - -
IL4 stimulation - - - - + +

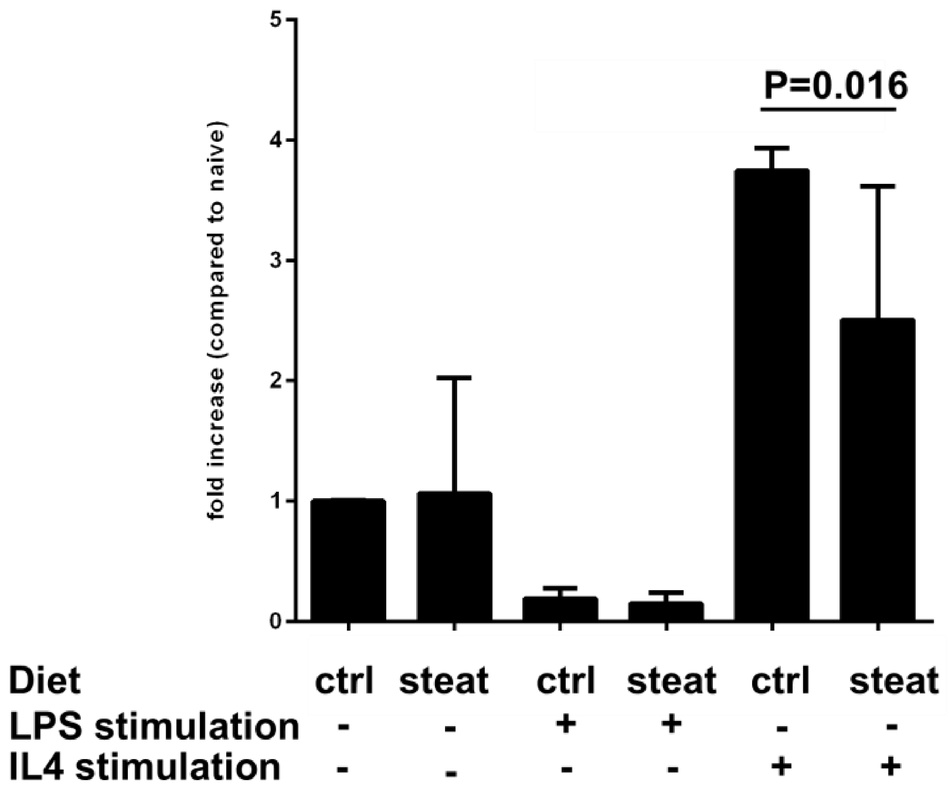
CD206
P=0.016
fold increase (compared to naive)
5
4
3
2
1
0
Diet
ctrl steat ctrl steat ctrl steat
LPS stimulation - - + + - -
IL4 stimulation - - - - + +

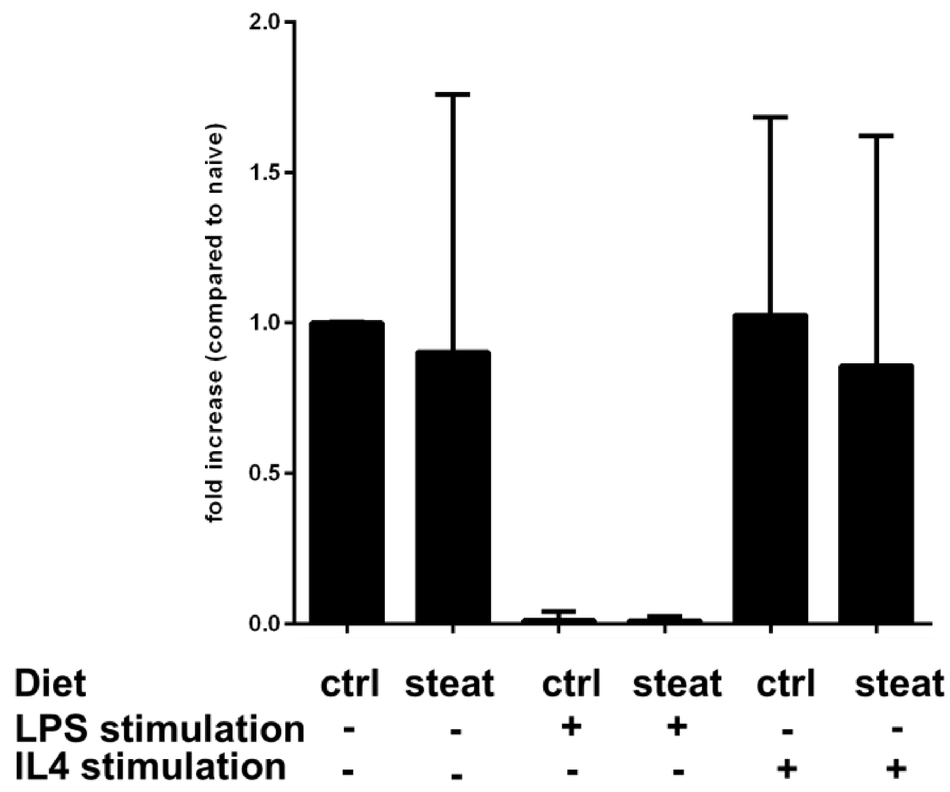
CD163
fold increase (compared to naive)
2.0
1.5
1.0
0.5
0.0
Diet
ctrl steat ctrl steat ctrl steat
LPS stimulation - - + + - -
IL4 stimulation - - - - + +

Figure 3

A **Phagocytosis, confocal microscopy (in vitro)**

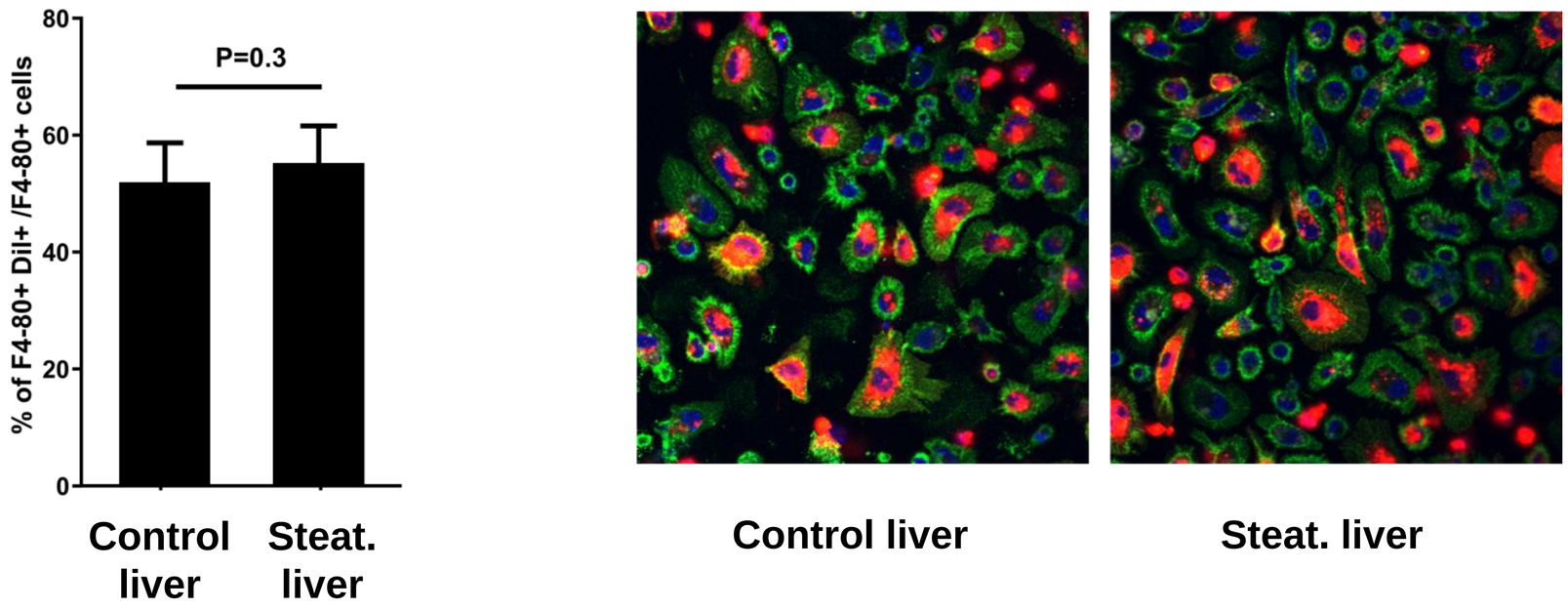

B **Phagocytosis, FACS analysis (in vitro)**

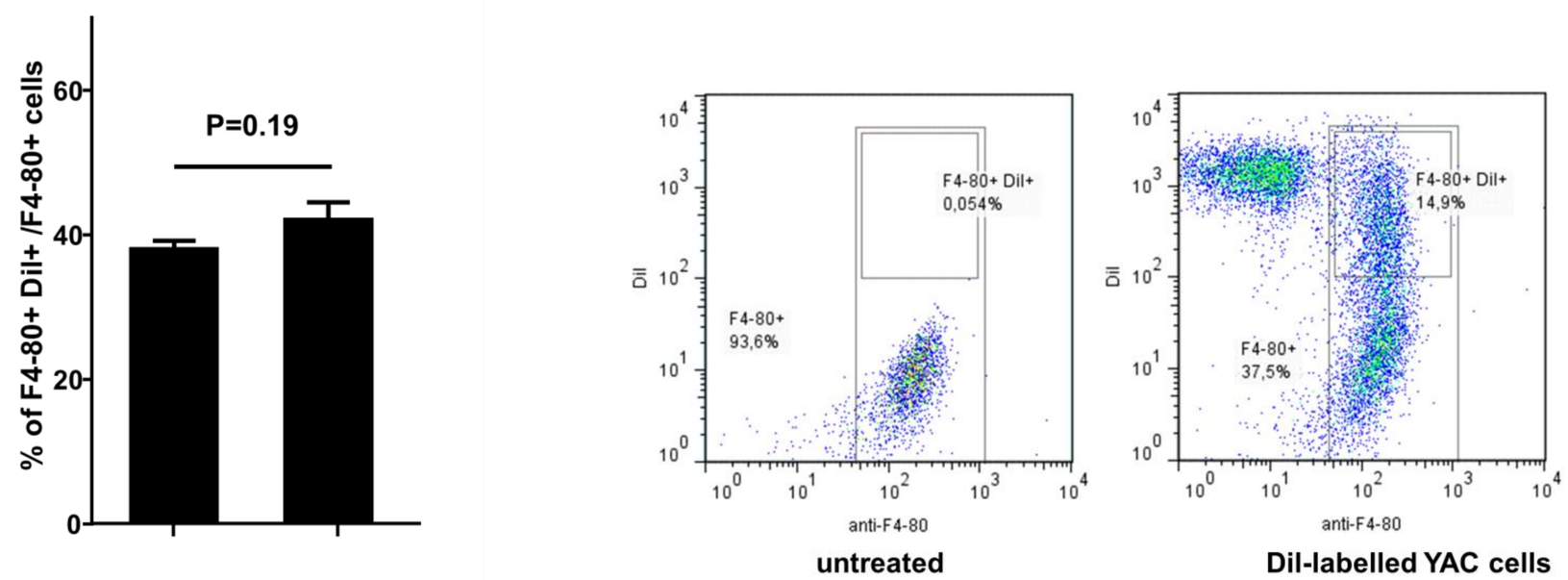

C **Phagocytosis, FACS analysis (in vivo)**

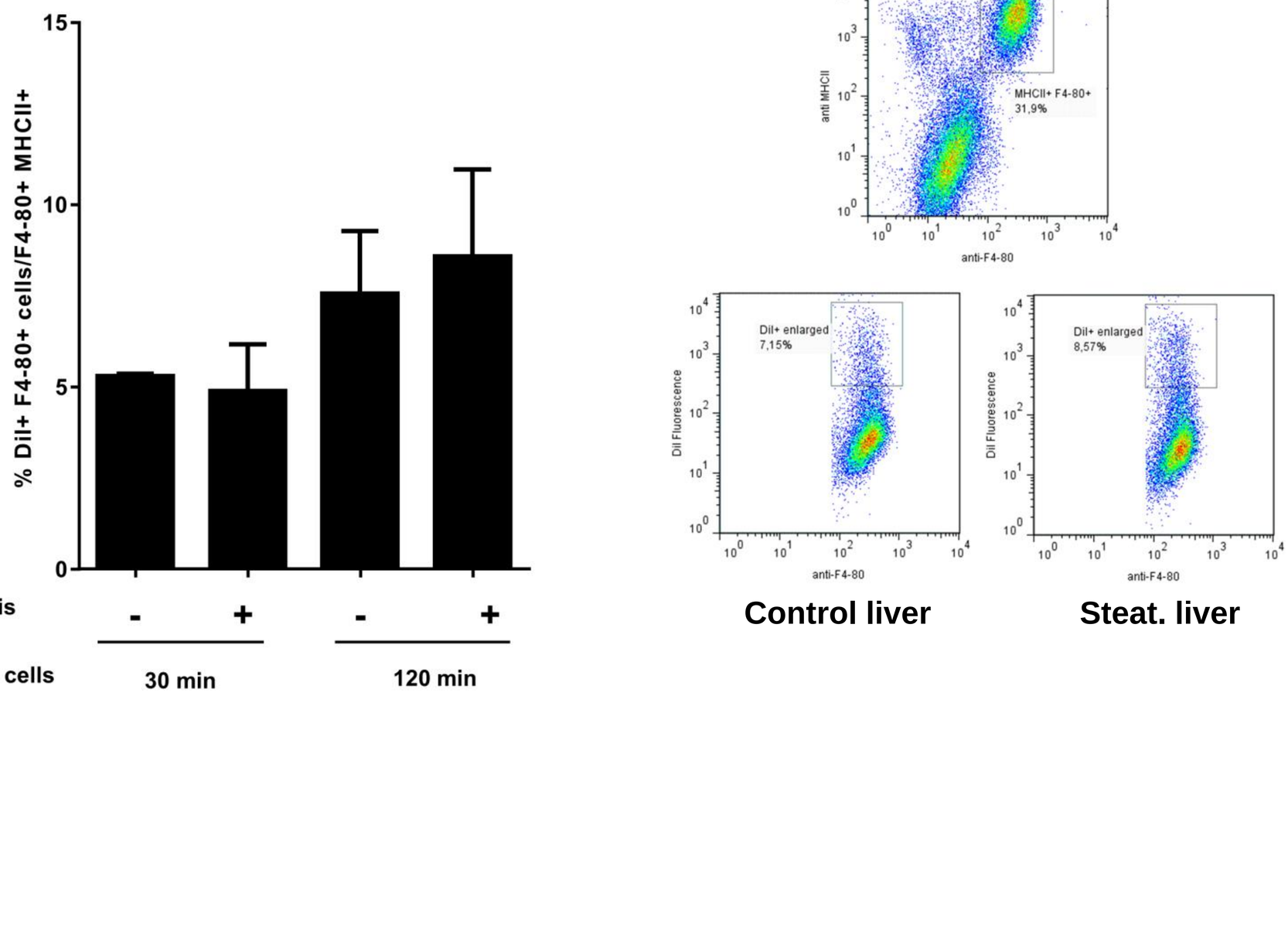

Figure 4

A

Diet-induced NASH model

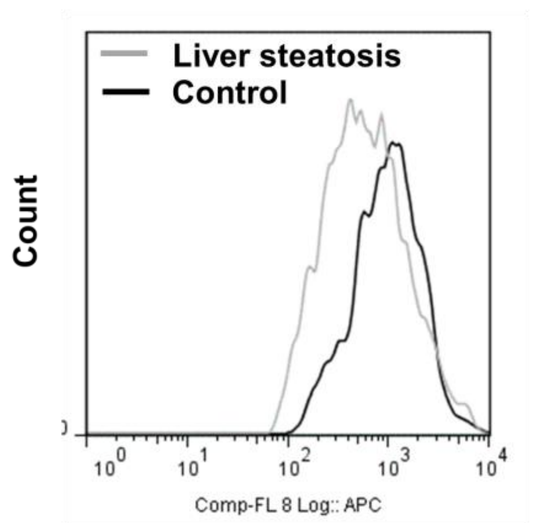

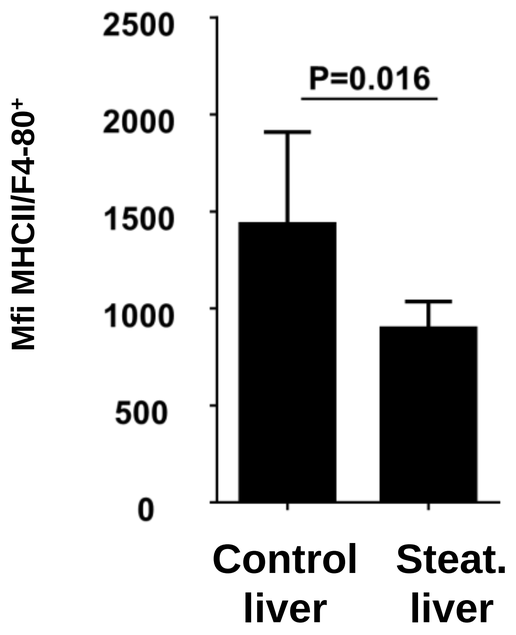

CCL4 model

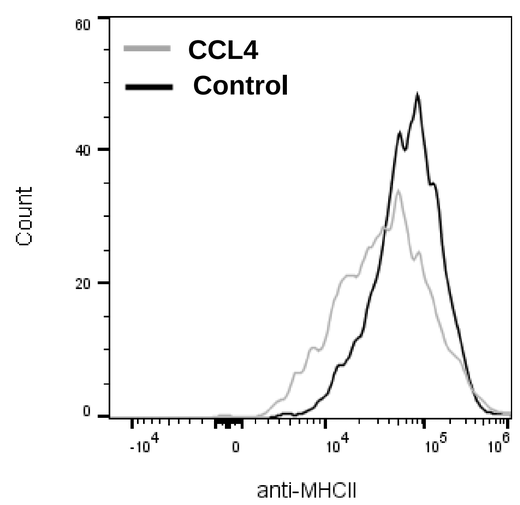

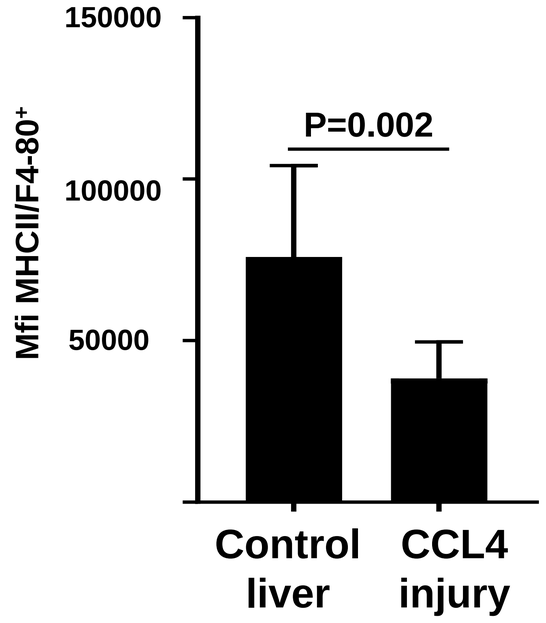

B

Diet-induced NASH model

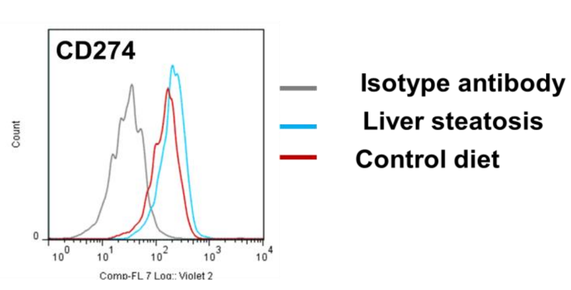

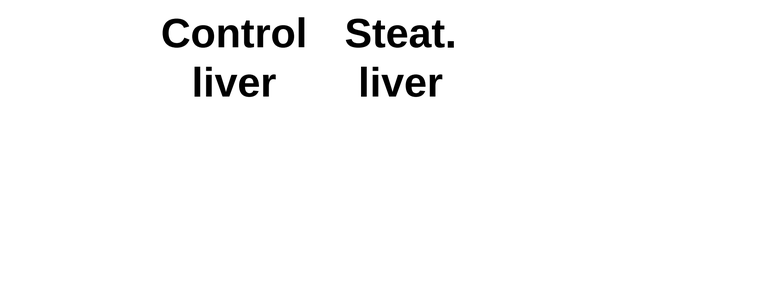

CCL4 model

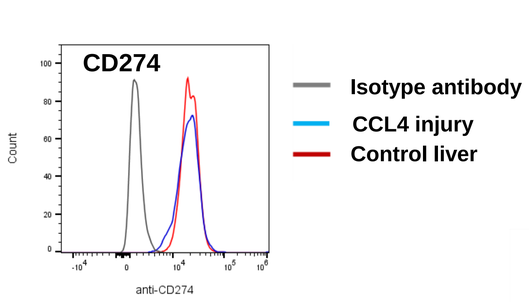

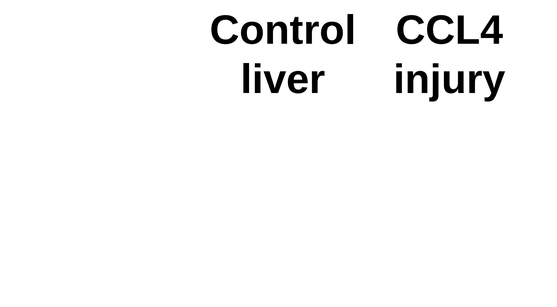

C

Diet-induced NASH model

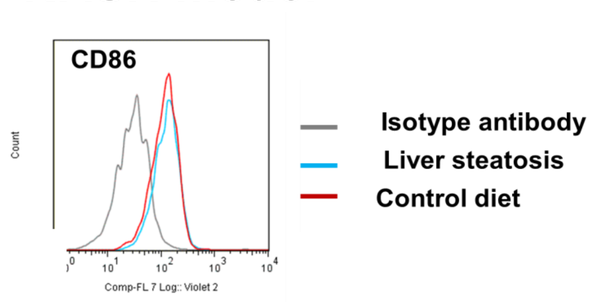

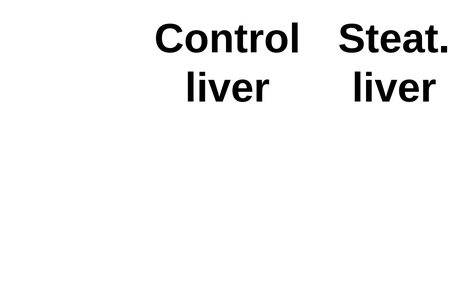

CCL4 model

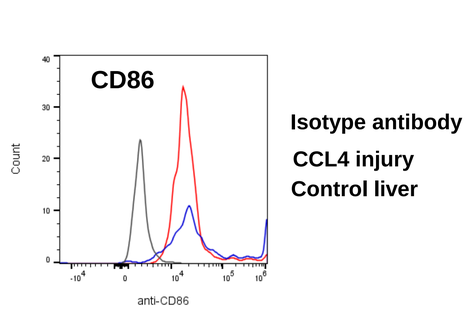

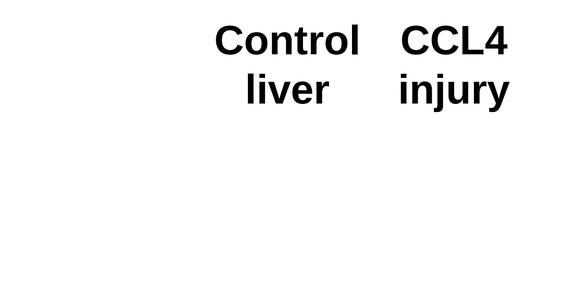

Figure 5

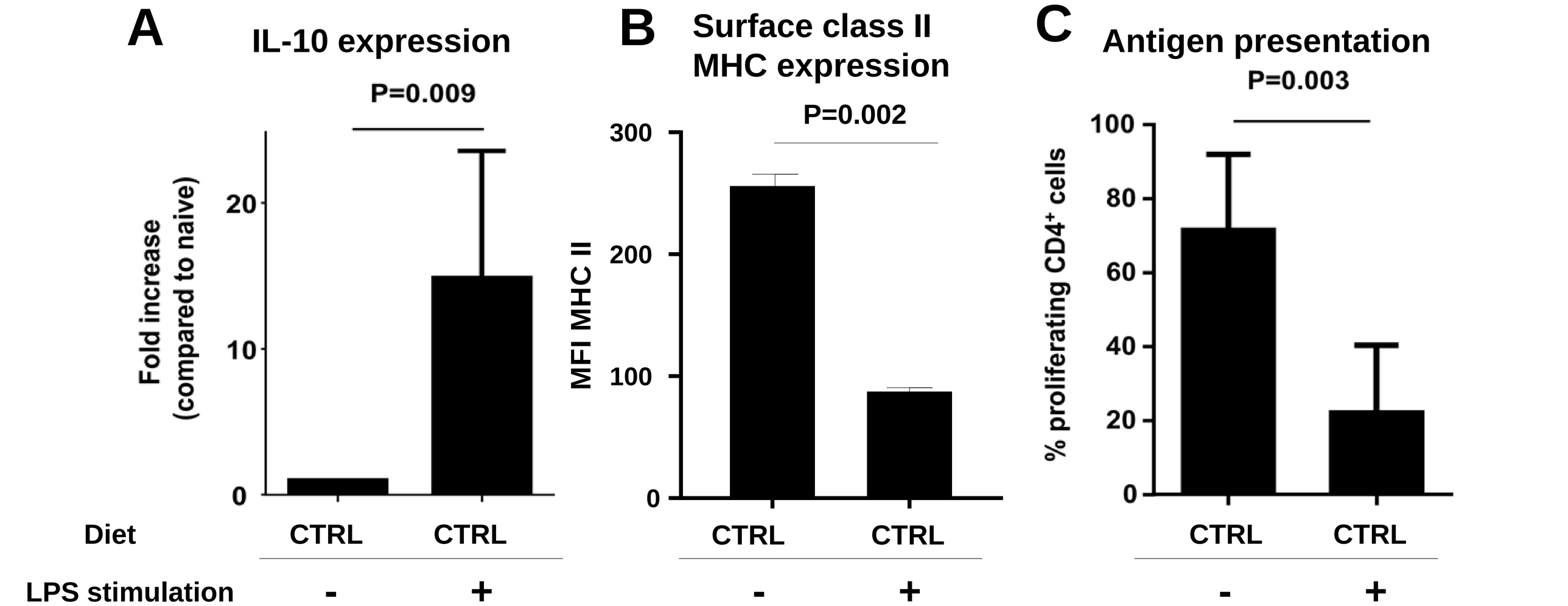
A
IL-10 expression
P=0.009
Fold increase (compared to naive)
20
10
0
B
Surface class II MHC expression
P=0.002
MFI MHC II
300
200
100
0
C
Antigen presentation
P=0.003
% proliferating CD4+ cells
100
80
60
40
20
0
Diet
CTRL
CTRL
CTRL
CTRL
CTRL
CTRL
LPS stimulation
-
+
-
+
-
+

Figure 6

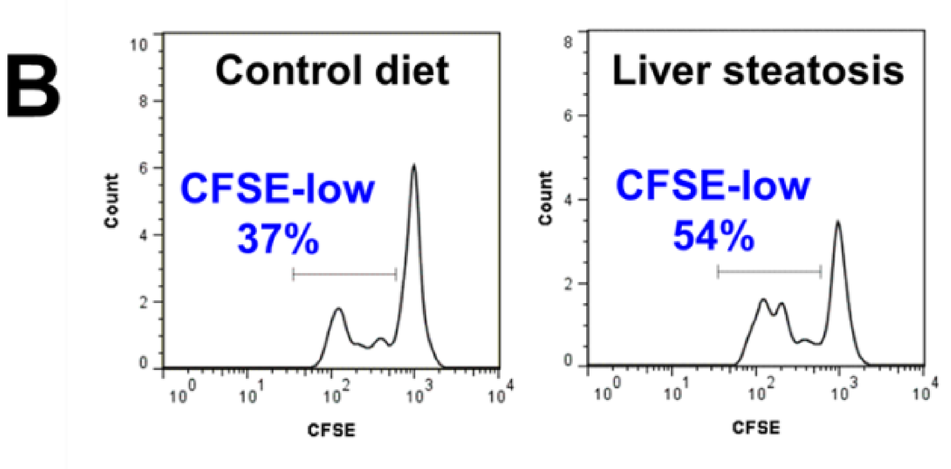
B
Control diet
CFSE-low
37%
Liver steatosis
CFSE-low
54%
Count
CFSE

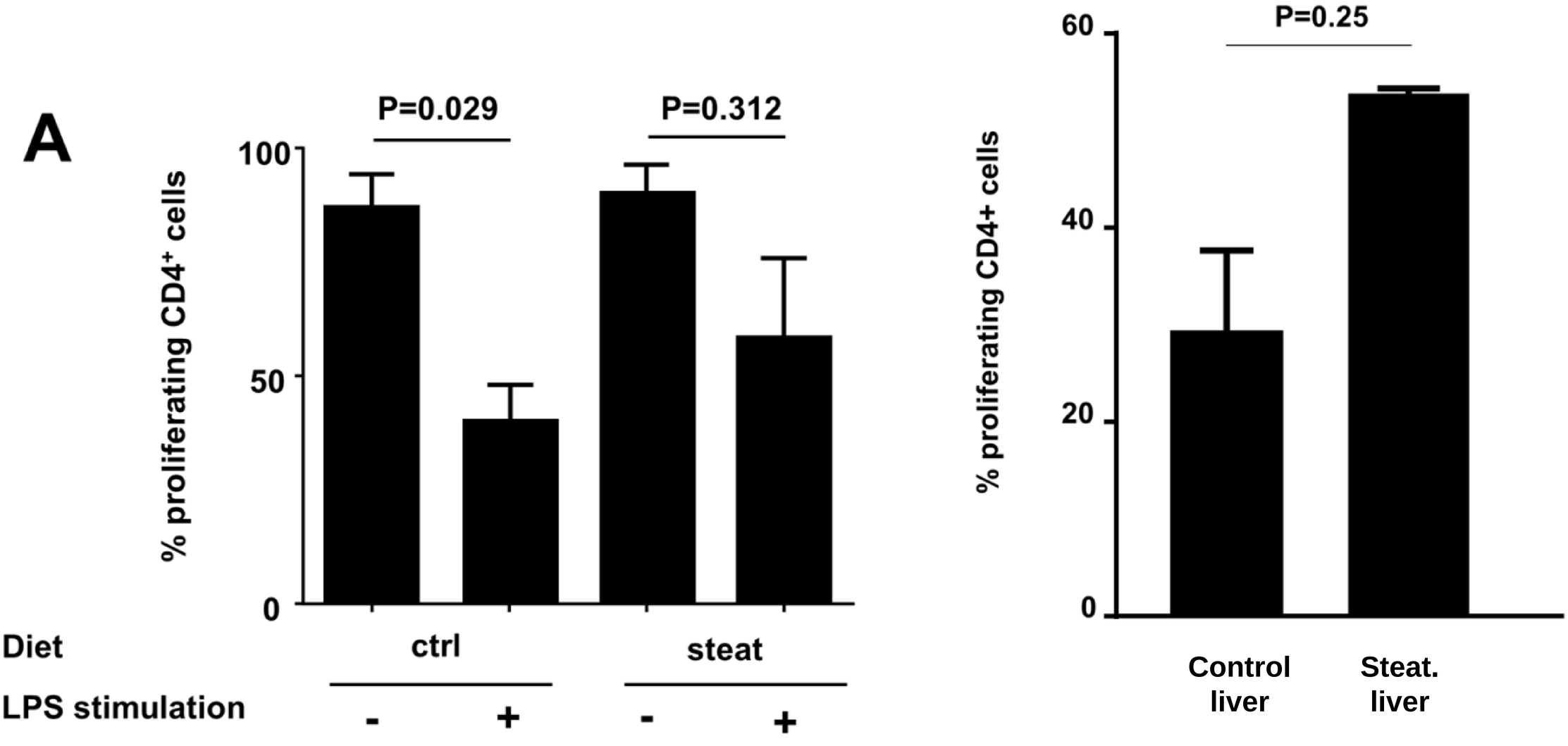
A
P=0.029
P=0.312
% proliferating CD4+ cells
Diet
ctrl
steat
LPS stimulation
- + - +
P=0.25
% proliferating CD4+ cells
Control liver
Steat. liver

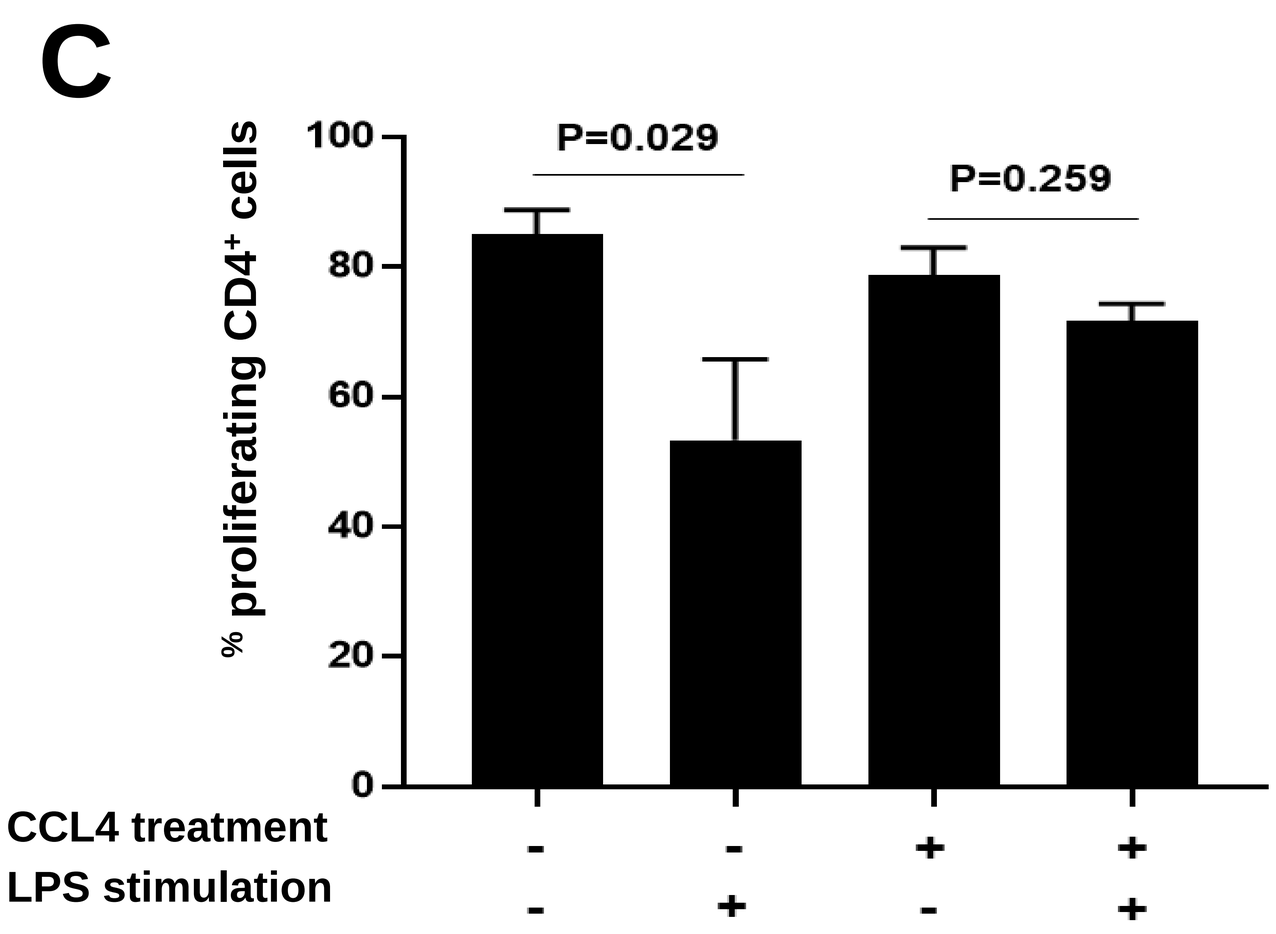
C
P=0.029
P=0.259
% proliferating CD4+ cells
CCL4 treatment
LPS stimulation
- - + +
- + - +

Figure 7

A

Class II MHC

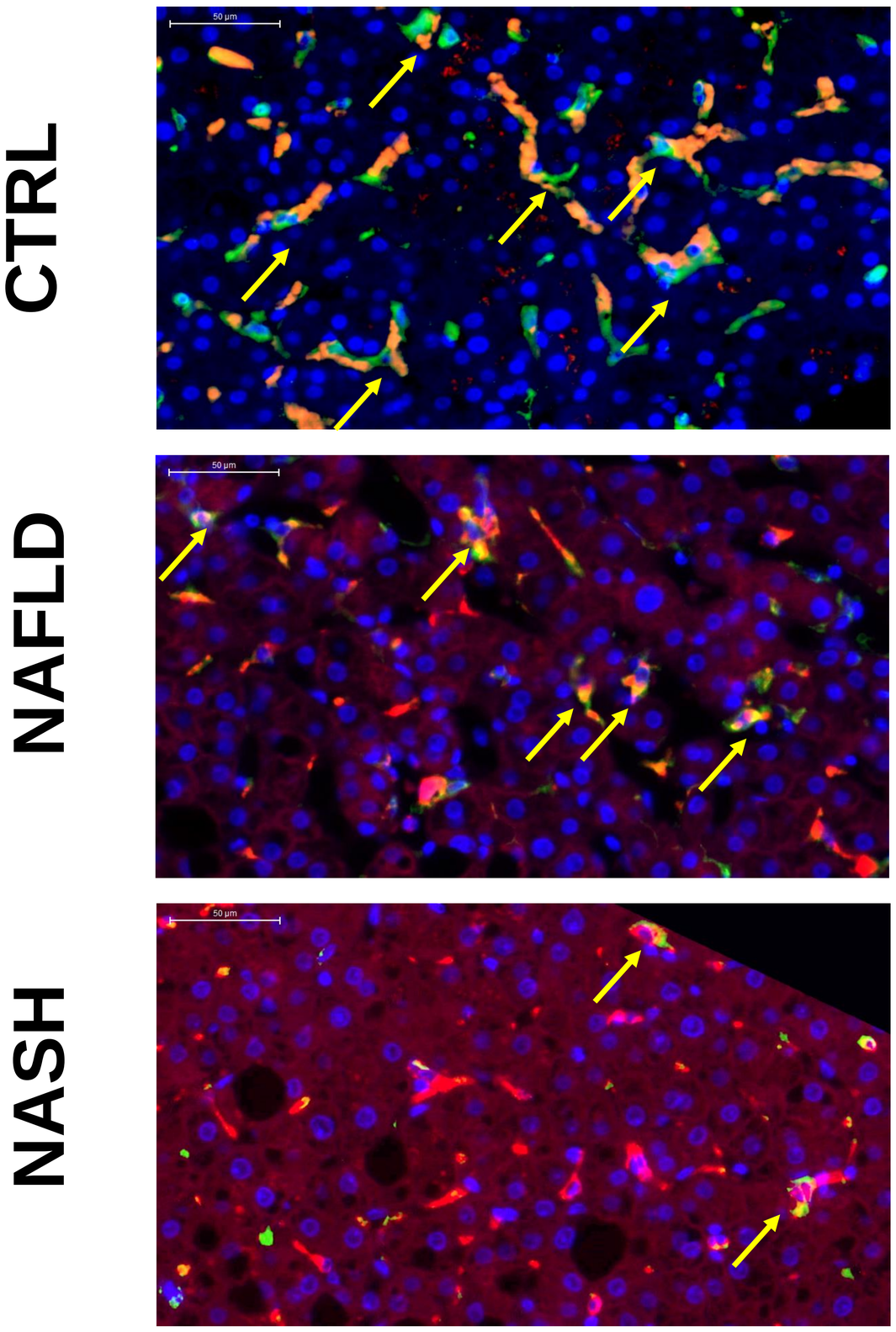

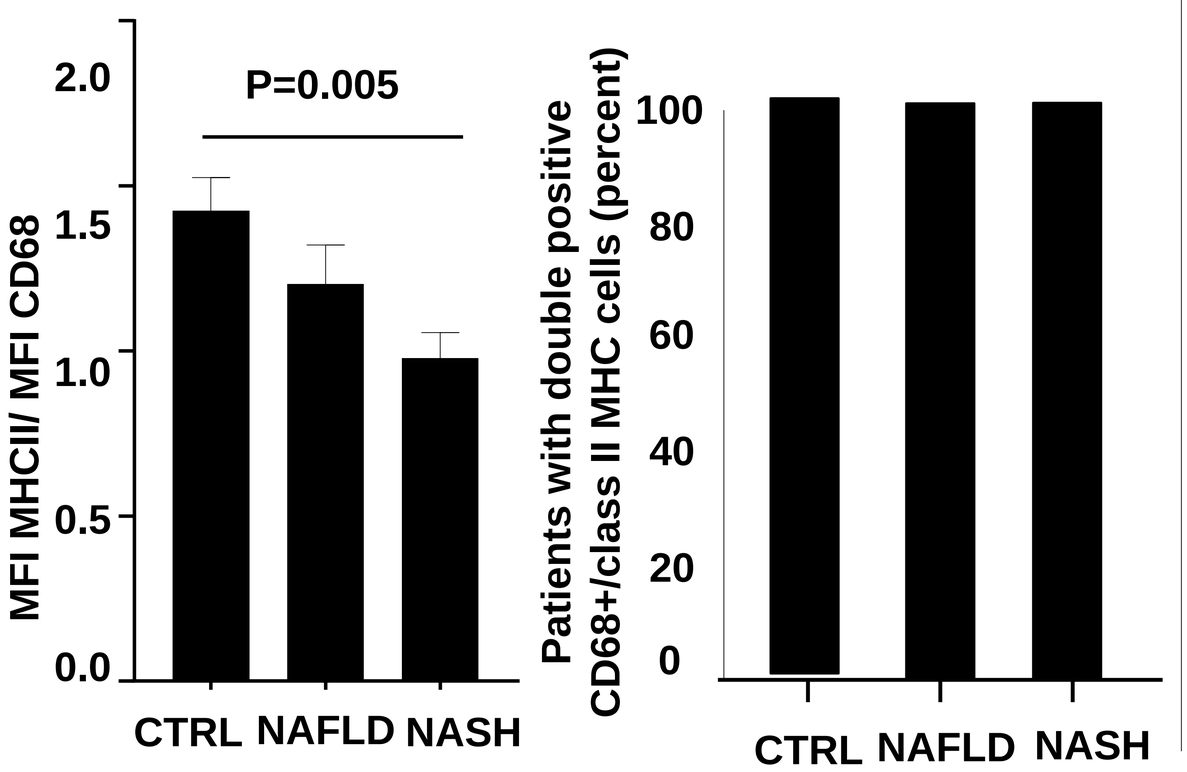

B

PD-L1